RADIO SCIENCE, VOL. 41, RS2S03, doi:10.1029/2005RS003431, 2006

Three-dimensional finite difference time domain modeling of the Schumann resonance parameters on Titan, Venus, and Mars

Heng Yang,[1] Victor P. Pasko,[1] and Yoav Yair[2]

Received 29 November 2005; revised 27 March 2006; accepted 17 May 2006; published 27 September 2006.

[1] The conducting ionosphere and conducting surface of Titan, Venus, and Mars form a concentric resonator, which would support the possibility of the existence of global electromagnetic resonances. On Earth, such resonances are commonly referred to as Schumann resonances and are excited by lightning discharges. The detection of such resonances on other planets would give a support for the existence of the electrical discharges in the lower atmosphere on these planets. In this paper, a three-dimensional finite difference time domain modeling for the extremely low frequency propagation is employed to study the Schumann resonance problems on Titan, Venus, and Mars. The atmospheric conductivity profiles for these studies are derived from the previously reported ionospheric models for these planets. The Schumann resonance frequencies and Q factors on these planets are calculated and are critically compared with those obtained from the previously published models.

Citation: Yang, H., V. P. Pasko, and Y. Yair (2006), Three-dimensional finite difference time domain modeling of the Schumann resonance parameters on Titan, Venus, and Mars, *Radio Sci.*, *41*, RS2S03, doi:10.1029/2005RS003431 [Printed *42*(2), 2007].

1. Introduction

[2] The combination of the highly conducting terrestrial surface boundary and the highly conducting ionospheric outer boundary separated by a weakly conducting atmosphere creates a spherically concentric cavity, the Earth-ionosphere cavity. The electromagnetic waves produced by global lightning activity are trapped in this cavity. The extremely low frequency (ELF, 3–3000 Hz) signals can travel around the Earth several times without suffering serious attenuation and produce resonances. The resonance properties of this cavity were first predicted by *Schumann* [1952], so these resonances are also called Schumann resonances (SR). The first experimental detection of Schumann resonances was presented by *Balser and Wagner* [1960].

[3] The analytical solution for the frequencies in the ideal cavity, which has the perfectly conducting ionosphere and ground boundaries, separated by free space, was given by *Schumann* [1952]:

$$f_n = \frac{c}{2\pi a}\sqrt{n(n+1)}, \tag{1}$$

where c is the speed of the light, a is the radius of the Earth, and n is the order of the resonance modes. In the realistic Earth-ionosphere cavity, the conductivity exponentially increases from the ground to the ionosphere because of the cosmic rays and solar radiation. The resonance frequencies in this cavity are less than those in the ideal cavity because of the conduction losses, and the first SR frequency is about 7.8 Hz [e.g., *Sentman*, 1995; *Nickolaenko and Hayakawa*, 2002].

[4] Since the discovery of SR, observations of ELF signals in the frequency range 1–50 Hz have been used in many remote sensing applications. The resonance parameters of a cavity are strongly related to the electromagnetic properties of the cavity. Therefore SR signals carry information on both sources and electromagnetic properties of the cavity determined by the lower ionospheric properties. Some inverse problem solutions have been developed for revealing the global lightning distribution and the planetary conductivity variation based on the analysis of the average background SR signals [e.g., *Heckman et al.*, 1998; *Cummer*, 2000; *Shvets*, 2001]. Because of the possible

[1]Communications and Space Sciences Laboratory, Pennsylvania State University, University Park, Pennsylvania, USA.
[2]Department of Natural Sciences, Open University, Ra'anana, Israel.

0048-6604/06/2005RS003431$11.00

connections between the Earth's climate and global lightning activity, SR observations can be also applied to monitor the global environmental changes. *Williams* [1992] employs SR as a global tropical thermometer based on measurements of SR reflecting total world-wide lightning activity and its connection with average tropical surface temperature. In addition, the monitoring of SR might provide a convenient method for tracking upper-tropospheric water-vapor variability and hence contribute to a better understanding of the processes affecting climate change [*Price*, 2000].

[5] In recent years, there has been an increasing interest in exploration of other planets of the solar system. Lightning discharges play an important role in the chemistry, energetics and dynamics of planetary atmospheres. Apart from the Earth, they have been detected on other planets either by direct imaging of the optical emissions from flashes emanating through the atmosphere or else by picking-up electromagnetic signals such as sferics or whistlers guided by the planet's magnetosphere (see extensive review by *Desch et al.* [2002]). On Venus, lightning activity have been deduced on the basis of the VLF emission detected by the Soviet landers Venera 11 and 12 [*Ksanfomaliti*, 1980], but the data from top-side observations by various spacecraft have not shown un-equivocal optical or electromagnetic signatures [*Russel*, 1993; *Gurnett et al.*, 2001]. Since there is no constant magnetic field on Venus, the electromagnetic power cannot be guided through the bulk of ionosphere outside the global electromagnetic cavity, which may be the reason why such signals cannot be detected outside the atmosphere of Venus. Probably, the same result could be expected on Titan having no constant magnetic field (A. P. Nickolaenko, private communication, 2006). There is little doubt, however, on the basis of the Voyager, Galileo and Cassini missions, that lightning discharges are prevalent on Jupiter [*Magalhães and Borucki*, 1991] and Saturn [*Gurnett et al.*, 2005], and that lightning is also believed to occur on Uranus [*Zarka and Pedersen*, 1986] and Neptune [*Kaiser et al.*, 1991]. Titan is also considered as a probable harbor of lightning activity [*Tokano et al.*, 2005], and the dust storms of Mars have been modeled to display electrostatic activity [*Farrell et al.*, 1999]. There have been a number of publications on studies of SR problems on these planets [e.g., *Nickolaenko and Rabinowicz*, 1982; *Sentman*, 1990b; *Pechony and Price*, 2004]. There are two important factors, which would facilitate the existence of Schumann resonance phenomenon on a planet. One is that the planet surface and the ionosphere should have high enough conductivity to reflect the electromagnetic waves and form a planetary resonant cavity for the propagation of the electromagnetic waves. The other is the existence of the electrical discharges within this cavity, which can be considered as the sources of the electromagnetic waves. We note that *Sentman* [1990b] provided a method to evaluate the SR parameters for the planets, which lack solid surface, e.g., Jupiter.

[6] On 14 January 2005, the Huygens probe landed on Titan, and started exploration of this largest moon of Saturn. One of multiple missions of Huygens probe is to detect if there are electric discharges in Titan's atmosphere and to explore the electromagnetic properties of Titan's lower ionosphere during its descent [*Grard et al.*, 1995; *Fulchignoni et al.*, 2005]. If SR were detected on Titan, they would provide a good support for the existence of the electrical discharges in the lower atmosphere on Titan, and the SR parameters are also useful in the study of the electromagnetic properties of Titan's lower ionosphere.

[7] Several reports about the application of the finite difference time domain (FDTD) method to solution of VLF/ELF propagation problems in the Earth-ionosphere cavity have recently appeared in the literature [e.g., *Pasko et al.*, 1998; *Thevenot et al.*, 1999; *Cummer*, 2000; *Berenger*, 2002; *Simpson and Taflove*, 2002, 2004; *Otsuyama et al.*, 2003; *Yang and Pasko*, 2005, 2006; *Soriano et al.*, 2005]. A finite difference method has been developed by *Ando et al.* [2005] to analyze the SR problems and to reconstruct the lightning distribution in the Earth-ionosphere cavity. *Nickolaenko et al.* [1999, 2004] and *Nickolaenko and Rabinowicz* [2001] gave an analytical solution for the ELF pulses from the lighting strokes in the time domain. In our previous work [*Yang and Pasko*, 2005], a three-dimensional (3-D) FDTD model is developed to describe the ELF propagation in the Earth-ionosphere cavity and the variation of SR parameters during solar proton events and X-ray bursts. In this paper, we use this FDTD model to extend our study to other celestial bodies, e.g., Titan, Venus, and Mars. By using the previously reported ionospheric models, the SR parameters on these celestial bodies are calculated. We critically compare our FDTD results with previous modeling results on related subjects available in the literature [e.g., *Nickolaenko and Rabinowicz*, 1982; *Pechony and Price*, 2004].

2. Model Formulation

2.1. 3-D FDTD Modeling for a Planetary Resonant Cavity

[8] In this paper, a 3-D FDTD model is employed to solve the ELF problems in a planetary resonant cavity. A simplified version of this model was previously applied to the Earth-ionosphere cavity by *Yang and Pasko* [2005]. The number of FDTD cells in θ and ϕ directions are 20 and 40, respectively. In r direction, the grid size is chosen to be 5 km. The cavity is excited by a vertical lightning current with 5 km length, which has a linear risetime 500 μs and exponential fall with timescale 5 ms. The reported results

for frequencies <40 Hz are not sensitive to the specifics of the chosen lightning current waveform.

[9] The SR eigenfrequencies and Q factors of the cavity are evaluated using Prony's method by fitting the time domain data with complex polynomials, $\sum_{i=1}^{n} A_i \exp(j\omega_i t)$ [*Hildebrand*, 1956, p. 379; *Füllekrug*, 1995], where A_i are the complex amplitudes of the resonances, and ω_i indicate the complex propagation parameters. The SR eigenfrequencies and Q factors of the cavity can be defined by $Re(\omega_i)/2\pi$ and $Re(\omega_i)/2Im(\omega_i)$, respectively.

2.2. Conductivity Profiles

[10] We employ three different uniform conductivity profiles to describe Titan's lower ionosphere. The first one is a "knee" model approximation (shown in Figure 1) originally introduced by *Mushtak and Williams* [2002]. The "knee" model is formulated as

$$\sigma(z) = \begin{cases} \sigma_{kn} \exp[(z - h_{kn})/\xi_b] & z < h_{kn} \\ \sigma_{kn} \exp[(z - h_{kn})/\xi_a] & z > h_{kn}, \end{cases} \quad (2)$$

where $\sigma_{kn} = 1.23 \times 10^{-8}$ S/m, $h_{kn} = 75.0$ km, $\xi_a = 29.0$ km, and $\xi_b = 10.9$ km [*Pechony and Price*, 2004]. Other two conductivity profiles on Titan used in this paper are taken from *Borucki et al.* [1987] and *Molina-Cuberos et al.* [2004] (shown in Figure 2). Because of the attachment of the ions and electrons to the cloud particles in Titan's atmosphere, the conductivity profile including the clouds (dashed line in Figure 2) is much smaller than that without including the clouds (solid line in Figure 2) below 400 km. For the arbitrary conductivity profiles like those shown in Figure 2, the FDTD method allows robust and easy solution of SR problems.

[11] *Borucki et al.* [1982] reported the conductivity profile on Venus below an altitude of 80 km. Because cloud and haze particles attach ions at around the altitude of 50 km, the conductivity is reduced in this region, and discontinuity of conductivity appears around 50 km. Such a profile cannot be approximated by a "knee" model profile, so a "double-knee" model developed by *Pechony and Price* [2004] is employed. The "double-knee" profile is formulated as

$$\sigma(z) = \begin{cases} \sigma_1 \exp[(z - h_1)/\xi_1] & z < h_1 \\ \sigma_2 \exp[(z - h_2)/\xi_2] & z > h_2, \end{cases} \quad (3)$$

where σ_1, σ_2 are conductivities at two "knee" altitudes h_1 and h_2, ξ_1 and ξ_2 are the scale heights of the conductivity below first and above second knee, respectively. The conductivity between altitude h_1 and h_2 is given by

$$\sigma(z) = \exp\left[\frac{z[\ln(\sigma_1) - \ln(\sigma_2)] + (h_1 \ln(\sigma_2) - h_2 \ln(\sigma_1))}{h_1 - h_2}\right], \quad (4)$$

where $h_1 < z < h_2$. The parameters determining the conductivity on Venus are shown in Table 1, and the conductivity profile is shown in Figure 3.

[12] *Sukhorukov* [1991] employs a two-exponential profile [*Greifinger and Greifinger*, 1978; *Sentman*, 1990a, 1996] to account for the conductivity profile on Mars (shown in Figure 4). In the development of SR theory, two-exponential profile plays a very important role. This profile is based on a division of the atmosphere into lower and upper layers with conductivity profiles

$$\sigma(z) = \begin{cases} \sigma(h_0) \exp[(z - h_0)/\xi_0] \\ \sigma(h_1) \exp[(z - h_1)/\xi_1], \end{cases} \quad (5)$$

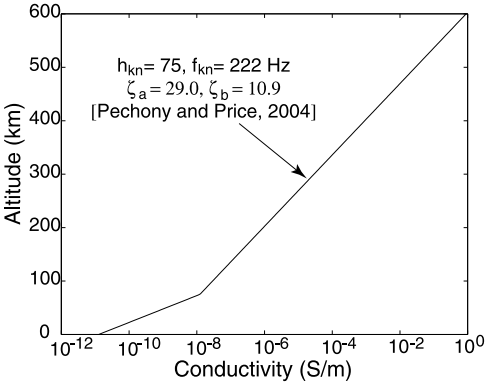

Figure 1. "Knee" model conductivity profile on Titan [*Pechony and Price*, 2004].

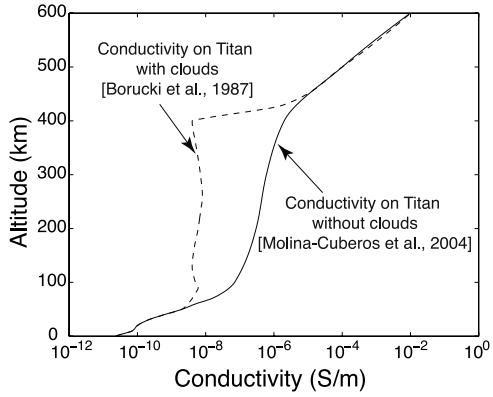

Figure 2. Conductivity profiles on Titan [*Borucki et al.*, 1987; *Molina-Cuberos et al.*, 2004].

Table 1. Conductivity Profile Parameters on Venus and Mars

	σ_1, S/m	σ_2, S/m	h_1, km	h_2, km	ξ_1, km	ξ_2, km
Venus	3.34×10^{-14}	5.57×10^{-15}	47.0	49.0	11.0	2.9
Mars (day)	8.35×10^{-9}	5.57×10^{-8}	28.0	53.0	3.5	4.6
Mars (night)	8.35×10^{-9}	5.57×10^{-8}	30.0	58.0	3.5	6.1

where h_0 = 53 km, ξ_0 = 6.0 km, h_1 = 100.0 km, ξ_1 = 4.8 km, $\sigma(h_0) = 2\pi f_0 \varepsilon_0 = 7.5 \times 10^{-10}$ S/m, and $\sigma(h_1) = 1/8\mu_0\pi f_0 \xi_1^2 = 1.02 \times 10^{-4}$ S/m assuming f_0 = 13.5 Hz [*Sukhorukov*, 1991].

[13] Another conductivity profile on Mars is taken from a partially uniform knee model (PUK) [*Pechony and Price*, 2004] (shown in Figure 5). The PUK model is principally different from the conductivity profiles discussed above, because it employs a nonuniform conductivity profile. The Martian conductivity on the day and night sides is assumed to have different distributions. For this purpose, in PUK model, two "double-knee" conductivity profiles with different parameters (shown in Table 1) are chosen. In the simulation, half planet is covered by day-time conductivity profile, and the other half is covered by nighttime conductivity profile. The specific choice of parameters for the profiles presented above is motivated by the availability of solutions of related SR problems [e.g., *Pechony and Price*, 2004], against which the FDTD results presented in this paper are compared.

3. Results and Discussion

3.1. Titan

[14] Figure 6 illustrates the time domain data of the E_r and H_ϕ components derived from our FDTD model for Titan conductivity profile shown in Figure 1. The distance between the source and the receiver is approximately 2400 km. Figure 7 indicates the vertical distributions of E_r and H_ϕ components for the first SR mode from the ground up to the altitude of 500 km. The E_r component remains constant below 40 km, which can be considered as the conducting boundary (defined by *Sentman* [1983, 1990a]) for the first SR mode. The H_ϕ component can penetrate to the altitude of approximately 300 km. The eigenfrequencies and Q factors are derived as described in section 2.1 by fitting the time domain data. In Figure 8a, a good agreement is found by comparing our FDTD results and the fitting data using Prony method on the H_ϕ component. Same values of the eigenfrequencies and Q factors can be calculated from the E_r components (not shown for the sake of brevity).

[15] Table 2 shows the comparison of our FDTD results for Titan and previous studies [*Morente et al.*, 2003; *Nickolaenko et al.*, 2003; *Pechony and Price*, 2004]. The frequencies and Q factors of the first three SR modes are given. Our FDTD results with "knee" model are close to the data reported by *Pechony and Price* [2004], and somewhat lower than values calculated by *Morente et al.* [2003]. A large difference is found with the frequencies predicted by *Nickolaenko et al.* [2003], which are approximately 2 times higher than our FDTD results. However, the Q factors obtained with FDTD model are within the range estimated by *Nickolaenko et al.* [2003].

[16] The conductivity profile (Figure 1) used in our FDTD model is taken from *Pechony and Price* [2004], which is very close to the profile used by *Morente et al.* [2003]. However, a 2–7 Hz difference in the first three

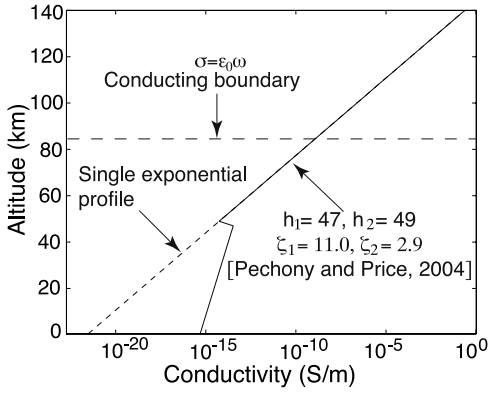

Figure 3. Conductivity profile on Venus [*Pechony and Price*, 2004].

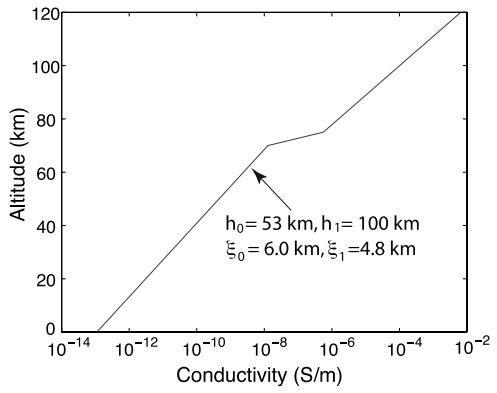

Figure 4. Conductivity profile on Mars [*Sukhorukov*, 1991].

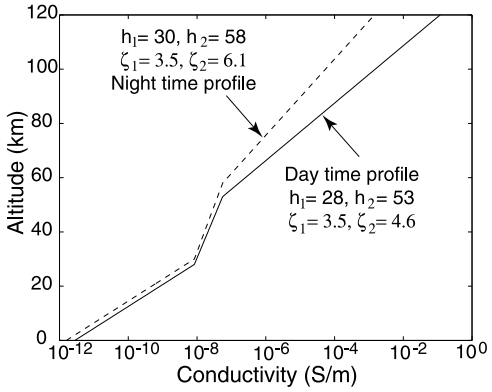

Figure 5. Conductivity profile on Mars [*Pechony and Price*, 2004].

modes is found between the results calculated by transmission line matrix method (TLM) [*Morente et al.*, 2003] and our FDTD model. It is believed that this difference comes from the different way to terminate the upper boundary of the cavity in these two models. *Morente et al.* [2003] locate the upper boundary of the Titan resonant cavity at about 180 km, where the conduction current is about one order of magnitude greater than the displacement current. At this altitude, the conductivity is approximately 10^{-7} S/m. We note that the conductivity around 10^{-7} S/m is not high enough to reflect most energy of the extremely low frequency wave. If the upper boundary is located at this altitude, a significant part of the dissipating region for ELF wave at higher altitudes is neglected, and the total energy dissipation in the cavity is reduced. Therefore the resonance frequencies and Q

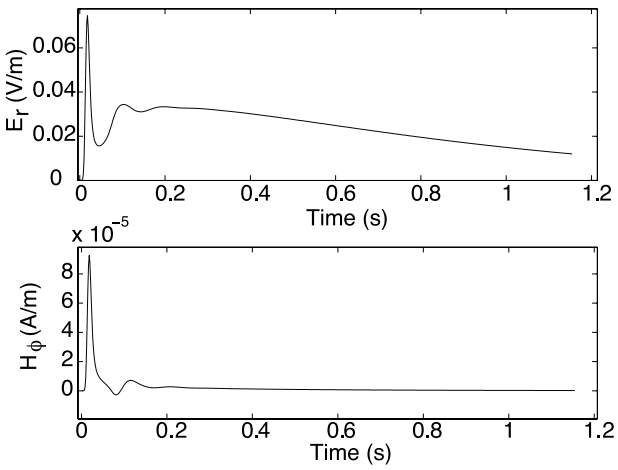

Figure 6. E_r and H_ϕ components in time domain derived by FDTD model for a case of the Titan conductivity profile shown in Figure 1.

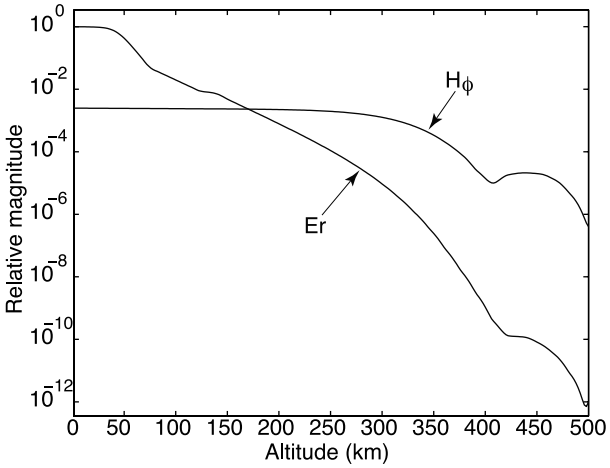

Figure 7. Vertical distribution of the magnitude of the E_r and H_ϕ components for the first SR mode on Titan with the conductivity profile shown in Figure 1.

factors derived from the TLM model [*Morente et al.*, 2003] appear to be higher than those obtained from FDTD model. We conducted additional tests to find the altitude where the upper boundary can be correctly placed without disturbing the electromagnetic properties of the resonant cavity. In the test simulations, a perfectly conducting surface was positioned at different altitudes, h. For h = 180 km, the corresponding first SR frequency is 13.1 Hz, which is close to the value 12.8 Hz, obtained by

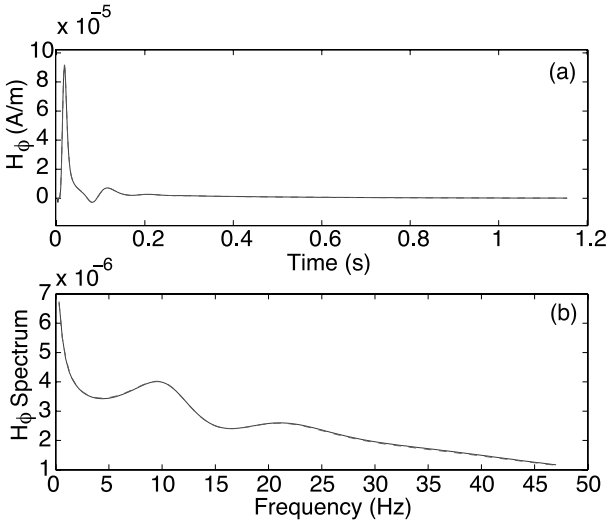

Figure 8. (a) Comparison of the FDTD result (dashed line) and the fitting data derived from Prony's method (solid line). (b) FFT results of the two time domain data shown in Figure 8a. Note that solid and dashed lines nearly coincide in both Figure 8a and Figure 8b.

Table 2. Schumann Resonances on Titan Calculated by Different Models

	TLM										
	Morente et al. [2003]	*Nickolaenko et al.* [2003]		PUK [*Pechony and Price*, 2004]		FDTD With "Knee" Model		FDTD With Profile From *Molina-Cuberos et al.* [2004]		FDTD With Profile From *Borucki et al.* [1987]	
Mode Number n	f_n	f_n	Q_n	f_n	Q_n	f_n	Q_n	f_n	Q_n	f_n	Q_n
1	12.8	19.9	0.96–2.6	11.8	1.8	10.6	1.40	8.2	0.92	9.4	1.04
2	24.4	35.8	0.97–2.7	22.5	1.9	20.5	1.49	17.4	0.99	14.3	0.82
3	38.1	51.8	1.01–2.8	34.1	2.0	30.8	1.54	27.3	1.06	31.4	1.23

Morente et al. [2003]. The first SR frequency decreases with increasing of the height h of the upper boundary above 180 km. When h is more than 500 km, the first SR frequency remains 10.4 Hz, and does not change any more with increasing h. It means that all of electromagnetic waves are reflected around or below the altitude of 500 km in Titan's atmosphere. Therefore the upper boundary should be located at the altitude of 500 km or higher in the simulations, rather than at 180 km employed by *Morente et al.* [2003]. Two conductivity profiles for Titan taken from *Molina-Cuberos et al.* [2004] and *Borucki et al.* [1987] (shown in Figure 2) are different from the model profile shown in Figure 1. In order to determine the correct altitude to place the upper boundary discussed above, we performed series of test runs in which a perfectly conducting surface was positioned at different altitudes above 180 km. It was determined that the first three SR frequencies derived from these two profiles (shown in Table 2) remain constant, when the upper boundary is positioned at 600 km or higher.

[17] *Nickolaenko et al.* [2003] derive the SR frequencies using the modified Greifinger's formula [e.g., *Nickolaenko and Rabinowicz*, 1982], which is given by

$$f_n = \frac{c}{2\pi a}\sqrt{n(n+1)}\sqrt{\frac{h_0}{h_1}}, \tag{6}$$

where h_0 is the altitude of the conducting boundary where the displacement current is equal to the conducting current at a given frequency f, namely, the conductivity at altitude h_0 is equal to $2\pi f\varepsilon_0$, and h_1 is the altitude of the reflection boundary defined by *Sentman* [1990a]. The h_0 and h_1 are related by equation (6) of *Nickolaenko et al.* [2003] as follows:

$$h_1 = h_0 - 2\xi_0 \ln(2k\xi_0), \tag{7}$$

where k is the wave number, and ξ_0 is the scale height of the conductivity profile at altitude h_0. This equation comes from equation (31) of *Greifinger and Greifinger* [1978], which is valid for a single exponential conductivity profile. Therefore the conductivity in the cavity is assumed to exponentially increase neglecting a "knee point" around 60 km. To illustrate this point, two single exponential profiles are employed in our FDTD model. The single exponential profile [*Galejs*, 1961] is given by

$$\sigma(z) = \sigma_0 \exp\left(\frac{z-G}{H}\right), \tag{8}$$

where G is the reference height and H is the scale height. The parameters are chosen to be the same as those in the Optimistic and Pessimistic models discussed by *Nickolaenko et al.* [2003]. The reference heights are 42 and 38 km, and the scale heights are 2.7 and 4.7 km, respectively, and $\sigma_0 = 5.55 \times 10^{-10}$ S/m. We found a good agreement on the SR frequencies between our FDTD model results and the data shown in Table 2 of *Nickolaenko et al.* [2003]. Therefore the large difference between *Nickolaenko et al.* [2003] and other models (see Table 2 of this paper) can be explained mainly by the different conductivity profiles used in these models.

3.2. Venus

[18] The first three SR frequencies and Q factors on Venus derived from three different models discussed in section 2.2 are shown in Table 3. A good agreement is found for the frequencies, with the difference generally not exceeding 3%. The Q factors derived from our FDTD model and those given by *Pechony and Price* [2004] are close to each other. These values, however, are approximately 2 times greater than the values calculated by *Nickolaenko and Rabinowicz* [1982]. The equation which was used to derive the Q factors of *Nickolaenko and Rabinowicz* [1982] is

$$Q_n = \frac{1}{\pi}\left(\frac{\xi_1}{h_1} + \frac{\xi_2}{h_2}\right)^{-1}, \tag{9}$$

where h_1 and h_2 are the altitudes of the conducting and reflection boundary, respectively, and ξ_1 and ξ_2 are the corresponding conductivity scale heights. In other papers [e.g., *Sentman*, 1990b, 1996], a similar equation used to derive Q factors is given by

$$Q_n = \frac{2}{\pi}\left(\frac{\xi_1}{h_1} + \frac{\xi_2}{h_2}\right)^{-1}. \tag{10}$$

Table 3. Schumann Resonances on Venus Calculated by Different Models

	Nickolaenko and Rabinowicz [1982]		PUK [*Pechony and Price*, 2004]		FDTD	
Mode Number n	f_n	Q_n	f_n	Q_n	f_n	Q_n
1	9.0	5.1	9.3	10.5	9.05	10.07
2	15.8	5.1	16.3	11.3	15.9	10.23
3	22.7	5.2	23.3	11.7	22.64	10.31

A factor of two difference between equations (9) and (10) is a likely reason for the observed difference in Q factors between our FDTD model and the analytical model presented by *Nickolaenko and Rabinowicz* [1982].

[19] The altitude where $\sigma = 2\pi\varepsilon_0 f$ can be considered as a conducting boundary (shown in Figure 3) for a specific frequency, f. The atmosphere below this boundary can be considered as insulating, whereas the atmosphere is conducting above this boundary [*Sentman*, 1990a, 1996]. For the first SR mode on Venus, the frequency, f, is approximately 10 Hz. The boundary between the conducting and nonconducting atmosphere therefore corresponds to the altitude where $\sigma = 2\pi\varepsilon_0 f = 5 \times 10^{-10}$ S/m. *Borucki et al.* [1982] reported only conductivity profile below 80 km on Venus, and the maximum value of the conductivity is approximately 10^{-10} S/m at 80 km. Therefore the region studied by *Borucki et al.* [1982] (below 80 km) can be considered as an insulating space for ELF waves, and the conductivity distribution in this region is not important for SR studies. *Pechony and Price* [2004] extended the conductivity to a higher altitude by a "double-knee" model. Since the SR parameters are only dependent on the conductivity distribution in the conducting region (above 80 km) in Venus-ionosphere cavity, which is determined by the reference height (h_2) and the scale height (ξ_2) in this "double-knee" model (see Table 1), it is believed that the nearly identical results can be obtained using both the "double-knee" model (solid line in Figure 3) and a single exponential conductivity profile (dashed line in Figure 3). We have performed additional simulations with single exponential conductivity profile with the same reference height ($G = 49$ km) and the scale height ($H = 2.9$ km) as those in the upper part of the "double-knee" model. As expected, the results appeared to be in a good agreement with those derived from the "double-knee" model. The flat frequency dependence of Q factors (last column in Table 3) also supports our conclusion, that the "double-knee" model shown in Figure 3 has the same effect on SR parameters as a single exponential profile. Readers are referred to additional discussion on related topics by *Mushtak and Williams* [2002] and *Yang and Pasko* [2005, and references therein].

3.3. Mars

[20] Table 4 shows the simulation results of the first three SR frequencies and Q factors for the resonant cavity on Mars. The first three SR frequencies predicted by *Sukhorukov* [1991] are approximately 13, 25, and 37 Hz, and the Q factors are between 3.3 and 4.0. These values appear to be substantially different from those calculated by *Pechony and Price* [2004]. The first three SR frequencies reported by *Pechony and Price* [2004] are 8.6, 16.3, and 24.4 Hz, and the Q factors are around 2.4. The observed differences can be explained by the different conductivity profiles used in these models as illustrated in Figures 4 and 5. *Pechony and Price* [2004] used a PUK model. The PUK model parameters and the conductivity profiles are shown in Figure 5. *Sukhorukov* [1991] employs a two-scale height profile (shown in Figure 4). FDTD simulations have been performed using these two conductivity models. The results are shown in Table 4. A good agreement is found between our FDTD results and results reported by *Sukhorukov* [1991] and *Pechony and Price* [2004] for the corresponding conductivity profiles. The results shown in the last column in Table 4 are the peak frequencies of the first three SR modes calculated recently by *Molina-Cuberos et al.* [2006] using TLM model [*Morente et al.*, 2003], in which the second and third modes have same frequencies. The peak frequency is defined as the frequency where the maximum power occurs. Because of the interference between the different modes in the resonant system, the peak frequencies deviate from the eigenfrequencies, and the deviation depends on the magnitude of each mode at the observation point. Therefore we can find the different peak frequencies at different locations in the cavity and on different wave components. In the work by *Molina-Cuberos et al.* [2006], the second and third modes form a single peak at 21.7 Hz because of the interference, and cannot be clearly distinguished. Therefore we conclude that the peak frequency is not suitable for the study of SR in a planetary resonant cavity with low Q factor, such as Mars and Titan. We note that efficient numerical techniques have been developed to calculate the SR parameters in the time domain and frequency domain, such as Lorentzian fitting [*Sentman*, 1987; *Mushtak and Williams*,

Table 4. Schumann Resonances on Mars Calculated by Different Models

Mode Number n	*Sukhorukov* [1991]		PUK [*Pechony and Price*, 2004]		FDTD With Conductivity Profile of *Sukhorukov* [1991]		FDTD With PUK		FDTD With Low-Conductivity Martian Crust		*Molina-Cuberos et al.* [2006]
	f_n	Q_n	f_n	Q_n	f_n	Q_n	f_n	Q_n	f_n	Q_n	f_n (Peak)
1	13–14	3.3–3.7	8.6	2.3	14.3	3.8	8.8	2.27	7.3	2.5	11.0
2	25–26	3.5–3.8	16.3	2.4	25.8	4.0	16.1	2.35	13.1	2.5	21.7
3	37–38	3.7–4.0	24.4	2.4	37.4	4.2	23.6	2.45	19.2	2.8	21.7

2002], the complex demodulation method [*Sátori et al.*, 1996], and Prony method [*Füllekrug*, 1995; *Yang and Pasko*, 2005, 2006], which allow accurate derivation of eigenfrequencies for low Q factor cavity. The Prony method, in particular, is employed for all calculations reported in the present paper (see section 2.1).

[21] To simplify the problem, the Martian crust is assumed to be perfectly conducting in the present paper. Although a low-frequency resonant cavity is roughly established for Mars, the low-conductivity upper Martian crust will be much less efficient as a boundary to reflect ELF waves than the surface of the Earth. The Martian surface does not hold a conductivity characteristic of the Earth shield (10^{-4} S/m) until depth of approximately 40–60 km [*Grimm*, 2002]. It means that the ELF waves can penetrate deeper into Martian crust than Earth shield, and ELF waves should suffer more attenuation during the propagation. We have performed some additional numerical experiments in which we inserted a low-conductivity layer below Martian surface to account for the Martian crust. The depth of this layer is 40 km, and the conductivity in this layer is 10^{-7} S/m [*Grimm*, 2002]. The first three SR frequencies decreased from 8.8, 16.1, and 23.6 Hz to 7.3, 13.1, and 19.2 Hz, respectively. The difference between the models with and without low-conductivity Martian crust is approximately 20% (see Table 4). Therefore the conductivity distribution of Martian crust from ground surface to the depth of 40–60 km is also an important factor determining the SR parameters on this planet. The measurements of the SR parameters can provide a good method to remotely sense the Martian subsurface conductivity profile to depths of 40–60 km, and locate anomalous conductivity structures in the Martian crust, such as mineral deposits and undergroundwater or ice [e.g., *Cummer and Farrell*, 1999; *Simpson and Taflove*, 2006].

3.4. Comparative Remarks

[22] Following equation (1), the SR frequencies are inversely proportional to the radius of the planet. Since the radius of Titan (2575 km) is approximately 40% of the Earth's radius (6370 km), the SR frequencies on Titan should be 2.5 times of those on Earth. However, the SR frequencies in these two cavities derived from our modeling are close to each other (see Table 2). It is important to emphasize that the conductivity distribution in a planetary resonant cavity is also an important factor which determines the SR frequencies, besides the radius of the planet. In Figure 7, the conducting boundary in Titan's atmosphere is around 40 km. The large region between this conducting boundary and the altitude of 500 km critically damps the ELF waves leading to the SR frequencies which are much lower than those predicted by equation (1) and also to the very low Q factor in the cavity. In Venus modeling (see section 3.2), the conducting boundary begins at 82 km. The small scale height of the Venusian conductivity above 82 km leads to a relatively sharp increase in the conductivity above this altitude allowing to terminate the cavity at 130 km. Therefore, on Venus, the dissipating region for ELF waves has much lower altitude extent than that on Titan. Therefore, on Venus, the Q factors are very high and the SR frequencies appear to be close to those calculated using equation (1).

4. Conclusions

[23] The main conclusions in this paper can be summarized as follows:

[24] 1. The first SR frequency on Titan is approximately 8–10 Hz, and the Q factor is around 0.9–1.4. The height of Titan-ionosphere cavity is about 500 km.

[25] 2. The first SR frequency on Venus is approximately 9 Hz, and the Q factor is around 10. The conductivity on Venus below 80 km is not important for the SR parameters.

[26] 3. The first SR frequency on Mars is approximately 8–9 Hz, and the Q factor is around 2.4. However, these SR parameters are also influenced by the conductivity distribution of Martian crust.

[27] **Acknowledgment.** This research was supported by NSF ATM-0134838 grant to Penn State University.

References

Ando, Y., M. Hayakawa, A. V. Shvets, and A. P. Nickolaenko (2005), Finite difference analyses of Schumann resonance and reconstruction of lightning distribution, *Radio Sci.*, *40*, RS2002, doi:10.1029/2004RS003153.

Balser, M., and C. A. Wagner (1960), Observations of Earth-ionosphere cavity resonances, *Nature*, *188*, 638.

Berenger, J. P. (2002), FDTD computation of VLF-LF propagation in the Earth-ionosphere waveguide, *Ann. Telecommun.*, *5*(11–12), 1059.

Borucki, W. J., Z. Levin, R. C. Whitten, R. G. Keesee, L. A. Capone, O. B. Toon, and J. Dubach (1982), Predicted electrical conductivity between 0 and 80 km in the Venusian atmosphere, *Icarus*, *51*, 302.

Borucki, W. J., Z. Levin, R. C. Whitten, R. G. Keesee, L. A. Capone, A. L. Summers, O. B. Toon, and J. Dubach (1987), Predictions of the electrical conductivity and charging of the aerosols in Titan's atmosphere, *Icarus*, *72*, 604.

Cummer, S. A. (2000), Modeling electromagnetic propagation in the Earth-ionosphere waveguide, *IEEE Trans. Antennas Propag.*, *48*(9), 1420.

Cummer, S. A., and W. M. Farrell (1999), Radio atmospheric propagation on Mars and potential remote sensing applications, *J. Geophys. Res*, *104*, 14,149.

Desch, S. J., W. J. Borucki, C. T. Russel, and A. Bar-Nun (2002), Progress in planetary lightning, *Rep. Prog. Phys.*, *65*, 955.

Farrell, W. M., M. L. Kaiser, M. D. Desch, J. G. Houser, S. A. Cummer, D. M. Wilt, and G. A. Landis (1999), Detecting electrical activity from Martian dust storms, *J. Geophys. Res.*, *104*(E2), 3795.

Fulchignoni, M., et al. (2005), In situ measurements of the physical characteristics of Titan's environment, *Nature*, *438*, 785.

Füllekrug, M. (1995), Schumann-resonances in magnetic-field components, *J. Atmos. Terr. Phys.*, *57*, 479.

Galejs, J. (1961), Terrestrial extremely low frequency noise spectrum in the presence of exponential ionospheric conductivity profiles, *J. Geophys. Res.*, *66*, 2789.

Grard, R., H. Svedhem, V. Brown, P. Falkner, and M. Hamelin (1995), An experimental investigation of atmospheric electricity and lightning activity to be performed during the descent of the Huygens probe onto Titan, *J. Atmos. Terr. Phys.*, *57*, 575.

Greifinger, C., and P. Greifinger (1978), Approximate method for determining ELF eigenvalues in the Earth-ionosphere waveguide, *Radio Sci.*, *13*, 831.

Grimm, R. E. (2002), Low-frequency electromagnetic exploration for groundwater on Mars, *J. Geophys. Res.*, *107*(E2), 5006, doi:10.1029/2001JE001504.

Gurnett, D. A., P. Zarka, R. Manning, W. S. Kurth, G. B. Hospodarski, F. T. Averkamp, M. L. Kaiser, and W. M. Farrell (2001), Non-detection at Venus of high-frequency radio signals characteristic of terrestrial lightning, *Nature*, *409*, 313.

Gurnett, D. A., et al. (2005), Radio and plasma wave observations at Saturn from Cassini's approach and first orbit, *Science*, *307*, 1255.

Heckman, S. J., E. Williams, and B. Boldi (1998), Total global lightning inferred from Schumann resonance measurements, *J. Geophys. Res.*, *103*(D24), 31,775.

Hildebrand, F. B. (1956), *Introduction to Numerical Analysis*, McGraw-Hill, New York.

Kaiser, M. L., P. Zarka, M. D. Desch, and W. M. Farrell (1991), Restrictions on the characteristics of Neptunian lightning, *J. Geophys. Res.*, *96*, 19,043.

Ksanfomaliti, L. (1980), Lightning in the cloud layer of Venus, *Cosmic Res.*, *17*(5), 617.

Magalhães, J. A., and W. J. Borucki (1991), Spatial distribution of visible lightning on Jupiter, *Nature*, *349*, 311.

Molina-Cuberos, G. J., J. Porti, B. P. Besser, J. A. Morente, J. Margineda, H. I. M. Lichtenegger, A. Salinas, K. Schwingenschuh, and H. U. Eichelberger (2004), Schumann resonances and electromagnetic transparence in the atmosphere of Titan, *Adv. Space Res.*, *33*, 2309.

Molina-Cuberos, G. J., J. A. Morente, B. P. Besser, J. Port, H. Lichtenegger, K. Schwingenschuh, A. Salinas, and J. Margineda (2006), Schumann resonances as a tool to study the lower ionospheric structure of Mars, *Radio Sci.*, *41*, RS1003, doi:10.1029/2004RS003187.

Morente, J. A., G. J. Molina-Cuberos, J. A. Porti, K. Schwingenschuh, and B. P. Besser (2003), A study of the propagation of electromagnetic waves in Titan's atmosphere with the TLM numerical method, *Icarus*, *162*, 374.

Mushtak, V. C., and E. Williams (2002), ELF propagation parameters for uniform models of the Earth-ionosphere waveguide, *J. Atmos. Sol. Terr. Phys.*, *64*, 1989.

Nickolaenko, A. P., and M. Hayakawa (2002), *Resonances in the Earth-Ionosphere Cavity*, Springer, New York.

Nickolaenko, A. P., and L. M. Rabinowicz (1982), On the possibility of existence of global electromagnetic resonances on the planets of solar system, *Space Res.*, *20*, 82.

Nickolaenko, A. P., and L. M. Rabinowicz (2001), Acceleration of the convergence of time domain presentations for the ELF pulses from the lighting strokes, *Telecommun. Radio Eng.*, *55*(5), 16.

Nickolaenko, A. P., M. Hayakawa, I. G. Kudintseva, S. V. Myand, and L. M. Rabinowicz (1999), ELF sub-ionospheric pulse in time domain, *Geophys. Res. Lett.*, *26*(7), 999.

Nickolaenko, A. P., B. P. Besser, and K. Schwingenschuh (2003), Model computations of Schumann resonance on Titan, *Planet. Space Sci.*, *51*, 853.

Nickolaenko, A. P., L. M. Rabinowicz, and M. Hayakawa (2004), Time domain presentation for ELF pulses with accelerated convergence, *Geophys. Res. Lett.*, *31*, L05808, doi:10.1029/2003GL018700.

Otsuyama, T., D. Sakuma, and M. Hayakawa (2003), FDTD analysis of ELF wave propagation and Schumann resonances for a subionospheric waveguide model, *Radio Sci.*, *38*(6), 1103, doi:10.1029/2002RS002752.

Pasko, V. P., U. S. Inan, T. F. Bell, and S. C. Reising (1998), Mechanism of ELF radiation from sprites, *Geophys. Res. Lett.*, *25*(18), 3493.

Pechony, O., and C. Price (2004), Schumann resonance parameters calculated with a partially uniform knee model on

Earth, Venus, Mars, and Titan, *Radio Sci.*, *39*, RS5007, doi:10.1029/2004RS003056.

Price, C. (2000), Evidence for a link between global lightning activity and upper tropospheric water vapour, *Nature*, *406*, 290.

Russel, C. T. (1993), Planetary lightning, *Annu. Rev. Earth Planet. Sci.*, *21*, 43.

Sátori, G., J. Szendröi, and J. Verö (1996), Monitoring Schumann resonances: I. Methodology, *J. Atmos. Terr. Phys.*, *58*, 1475.

Schumann, W. O. (1952), Uber die strahlungslosen einer leitenden Kugel die von einer Luftschicht und einer Ionospharenhulle umgeben ist, *Z. Naturforsch. A*, *7*, 149.

Sentman, D. D. (1983), Schumann resonance effects of electrical conductivity perturbations in an exponential atmospheric/ionospheric profile, *J. Atmos. Terr. Phys.*, *45*, 55.

Sentman, D. D. (1987), Magnetic elliptical polarization of Schumann resonances, *Radio Sci.*, *22*, 595.

Sentman, D. D. (1990a), Approximate Schumann resonance parameters for a 2-scale-height ionosphere, *J. Atmos. Terr. Phys.*, *52*, 35.

Sentman, D. D. (1990b), Electrical conductivity of Jupiter's shallow interior and the formation of a resonant planetary-ionospheric cavity, *Icarus*, *88*, 73.

Sentman, D. D. (1995), Schumann resonances, in *Handbook of Atomospheric Electrodynamics*, p. 267, CRC Press, Boca Raton, Fla.

Sentman, D. D. (1996), Schumann resonance spectra in a two-scale-height Earth-ionosphere cavity, *J. Geophys. Res.*, *101*, 9479.

Shvets, A. V. (2001), A technique for reconstruction of global lightning distance profile from background Schumann resonance signal, *J. Atmos. Sol. Terr. Phys.*, *63*, 1061.

Simpson, J. J., and A. Taflove (2002), Two-dimensional FDTD model of antipodal ELF propagation and Schumann resonance of the Earth, *Antennas Wireless Propag. Lett.*, *1*(2), 53.

Simpson, J. J., and A. Taflove (2004), Two-dimensional FDTD model of antipodal ELF propagation and Schumann resonance of the Earth, *IEEE Trans. Antennas Propag.*, *52*(2), 443.

Simpson, J. J., and A. Taflove (2006), A novel ELF radar for major oil deposits, *IEEE Geosci. Remote Sens. Lett.*, *3*(1), 36.

Soriano, A., E. A. Navarro, D. L. Paul, J. A. Porti, J. A. Morente, and I. J. Craddock (2005), Finite-difference time domain simulation of the Earth-ionosphere resonant cavity: Schumann resonances, *IEEE Trans. Antennas Propag.*, *53*(4), 1535.

Sukhorukov, A. I. (1991), On the Schumann resonances on Mars, *Planet. Space Sci.*, *39*, 1673.

Thevenot, M., J. P. Berenger, T. Monediere, and F. Jecko (1999), A FDTD scheme for the computation of VLF-LF propagation in the anisotropic Earth-ionosphere waveguide, *Ann. Telecommun.*, *54*(5–6), 297.

Tokano, T., G. J. Molina-Cuberos, H. Lammer, and W. Stumptner (2005), Modeling of thunderclouds and lightning generation on Titan, *Planet. Space Sci.*, *49*(6), 539.

Williams, E. R. (1992), The Schumann resonance—A global tropical thermometer, *Science*, *256*, 1184.

Yang, H., and V. P. Pasko (2005), Three-dimensional finite difference time domain modeling of the Earth-ionosphere cavity resonances, *Geophys. Res. Lett.*, *32*, L03114, doi:10.1029/2004GL021343.

Yang, H., and V. P. Pasko (2006), Three-dimensional finite difference time domain modeling of the diurnal and seasonal variations in Schumann resonance parameters, *Radio Sci.*, doi:10.1029/2005RS003402, in press.

Zarka, P., and B. M. Pedersen (1986), Radio detection of Uranian lightning by Voyager 2, *Nature*, *323*, 605.

V. P. Pasko and H. Yang, CSSL, Penn State University, 211B EE East, University Park, PA 16802, USA. (vpasko@psu.edu; hxy149@psu.edu)

Y. Yair, Department of Natural Sciences, Open University, Ra'anana, 43107, Israel. (yoavya@openu.ac.il)